


**Please cite the Published Version**

Ibrahim, Sabreen Waleed, Hamad, Thekra Ismael and Haider, Julfikar  (2023) Biological properties of polycaprolactone and barium titanate composite in biomedical applications. Science Progress, 106 (4). pp. 1-31. ISSN 0036-8504

**DOI:** <https://doi.org/10.1177/00368504231215942>

**Publisher:** SAGE Publications

**Version:** Published Version

**Downloaded from:** <https://e-space.mmu.ac.uk/633487/>

**Usage rights:**  [Creative Commons: Attribution-Noncommercial 4.0](https://creativecommons.org/licenses/by-nc/4.0/)

**Additional Information:** This is an open access article published in Science Progress, by SAGE Publications.

**Enquiries:**

If you have questions about this document, contact [openresearch@mmu.ac.uk](mailto:openresearch@mmu.ac.uk). Please include the URL of the record in e-space. If you believe that your, or a third party's rights have been compromised through this document please see our Take Down policy (available from <https://www.mmu.ac.uk/library/using-the-library/policies-and-guidelines>)

# Biological properties of polycaprolactone and barium titanate composite in biomedical applications

Science Progress

2023, Vol. 106(4) 1–31

© The Author(s) 2023

Article reuse guidelines:

[sagepub.com/journals-permissions](https://sagepub.com/journals-permissions)

DOI: 10.1177/00368504231215942

[journals.sagepub.com/home/sci](https://journals.sagepub.com/home/sci)

Sabreen Waleed Ibrahim<sup>1</sup> ,  
Thekra Ismael Hamad<sup>2</sup>  
and Julfikar Haider<sup>3</sup>

<sup>1</sup>Prosthodontic Department, College of Dentistry, Al Mustansiriyah University, Baghdad, Iraq

<sup>2</sup>Department of Prosthodontics, College of Dentistry, University of Baghdad, Baghdad, Iraq

<sup>3</sup>Department of Engineering, Manchester Metropolitan University, Manchester, UK

## Abstract

The ceramic-polymer composite materials are widely known for their exceptional mechanical and biological properties. Polycaprolactone (PCL) is a biodegradable polymer material extensively used in various biomedical applications. At the same time, barium titanate (BT), a ceramic material, exhibits piezoelectric properties similar to bone, which is essential for osseointegration. Furthermore, a composite material that combines the benefits of PCL and BT results in an innovative composite material with enhanced properties for biomedical applications. Thus, this review is organised into three sections. Firstly, it aims to provide an overview of the current research on evaluating biological properties, including antibacterial activity, cytotoxicity and osseointegration, of PCL polymeric matrices in its pure form and reinforced structures with ceramics, polymers and natural extracts. The second section investigates the biological properties of BT, both in its pure form and in combination with other supporting materials. Finally, the third section provides a summary of the biological properties of the PCLBT composite material. Furthermore, the existing challenges of PCL, BT and their composites, along with future research directions, have been presented. Therefore, this review will provide a state-of-the-art understanding of the biological properties of PCL and BT composites as potential futuristic materials in biomedical applications.

## Keywords

Barium titanate, polycaprolactone, composite, antibacterial, cytotoxicity, osseointegration

## Corresponding author:

Sabreen Waleed Ibrahim, Prosthodontic Department, College of Dentistry, Al Mustansiriyah University, Baghdad, Iraq.

Email: [sabreen87@uomustansiriyah.edu.iq](mailto:sabreen87@uomustansiriyah.edu.iq)



Creative Commons Non Commercial CC BY-NC: This article is distributed under the terms of the Creative Commons Attribution-NonCommercial 4.0 License (<https://creativecommons.org/licenses/by-nc/4.0/>)

which permits non-commercial use, reproduction and distribution of the work without further permission provided the original work is attributed as specified on the SAGE and Open Access page (<https://us.sagepub.com/en-us/nam/open-access-at-sage>).

## Introduction

Bone is a remarkable tissue with a great potential for regeneration following injury. Throughout history, numerous traditional medicinal practices across various cultures have been centered on bone regeneration. Despite significant advancements in biomaterials and medicine over the past few decades in managing bone defects, large bone defects still necessitate the insertion of bone grafts. Most of the time, cadaveric, autologous and xenogeneic tissue is used to create bone grafts; this carries a risk of transplant rejection and unfavourable inflammatory and immunological reactions. New treatments and medical equipment are being developed to enhance patient quality of life by preventing or minimising this type of response from the body. Tissue engineering aims to restore or regenerate damaged tissues and organs. The scaffolds have been mixed with bioactive agents, such as growth factors, to facilitate tissue growth and mimic the extracellular matrix.<sup>1,2</sup>

Natural or synthetic polymers, ceramics and their composite materials have been widely used as biomaterials, most frequently employed for building scaffolds and implant coating materials that support the formation of bone tissue.<sup>3-6</sup>

Synthetic biodegradable polymers find numerous applications in the field of biomedicine, while biopolymers are desirable materials for biomedical implants due to their high bioactivity, non-toxicity and resorbability properties. Furthermore, polymers can be considered 'smart' materials that have gained popularity as polymer coatings in various applications, such as corrosion resistance, surface functionalisation, wear resistance, enhancement of bioactivity and even switchable smart materials.<sup>7</sup> A crucial component of regenerative medicine is the creation of porous scaffolds from synthetic polymers that are biocompatible and biodegradable.<sup>8</sup>

Ceramic-polymer bioactive composites have been developed to integrate the inherent qualities of each component and optimise the physicochemical and biological properties required for complex tissue engineering. Such composite systems offer a degree of flexibility, favourable mechanical properties, enhanced biological activity and improved osteoconductivity when bioactive ceramics are combined with biodegradable polymers such as polycaprolactone (PCL), polyglycolic acid, polylactic acid (PLA) and their copolymers.<sup>9</sup>

While bioactive ceramics are biologically active and osteoconductive, they are also quite brittle and lack flexibility and moldability. As a result, their use has been limited to non-load-bearing sections. The ceramics must first undergo a high-temperature sintering to incorporate them into a bulk body. However, their brittleness makes the sintered part unsuitable for load-bearing locations. The density of bioceramics is also affected by sintering. Generally, densification eliminates pores acting as defects in the microstructure. Although the high-temperature treatment improves densification and reduces porosity, the bulk material may crack. High porosity promotes corrosion and releases material ions induced by the body's environment. Reduction of porosity by high temperature promotes cracks that might result from the difference in thermal coefficients of materials. This affects the expansion and shrinkage differences between the composite materials at heating and cooling during the sintering process, thus resulting in thermal stress.<sup>10</sup> Combining bioactive ceramics with flexible and moldable polymers is, therefore, one

of the most effective ways to create integrated ceramics that are easy to handle.<sup>11</sup> A concern when using polymers in the *in vivo* condition is the acidic environment created during their degradation, which can lead to inflammatory issues. Therefore, ceramic buffering fillers have been introduced to maintain a neutral pH level.<sup>12</sup>

The qualities of ceramics significantly impact the degradation rate and the mechanical and biological properties of ceramic/polymer composites.<sup>13</sup> This paper aims to investigate the antibacterial, cytotoxicity and osseointegration biological properties of ceramic material (barium titanate [BT]), polymer (PCL) and their composites.

## Polycaprolactone

Polycaprolactone belongs to the family of aliphatic polyesters and is a hexanoate repeat polymer. Its molecular weight and degree of crystallinity influence its thermal, mechanical and physical properties, affecting its ability to degrade under physiological conditions via hydrolysis of its ester bonds. Polycaprolactone is highly semicrystalline, hydrophobic, easily processable due to its low melting temperature, highly soluble at room temperature and exhibits excellent mix compatibility. As the molecular weight of PCL increases, its crystallinity tends to decrease.<sup>14,15</sup> The melting point of PCL is between 59°C and 64°C, and its glass transition temperature is -60°C. Polycaprolactone is soluble in solvents such as acetic acid, formic acid, benzene, carbon tetrachloride, chloroform, dichloromethane, toluene, 2-nitropropane and cyclohexanone at room temperature. Polycaprolactone is insoluble in diethyl ether and petroleum ether with low solubility in acetonitrile, acetone, ethyl acetate, 2-butanone and dimethylformamide (DMF). Because of its superior solubility properties, chloroform was the main solvent employed for PCL. The particles created with this solvent typically have small pores because of the quick evaporation of chloroform. However, the biomedical field has avoided employing this solvent as much due to concerns regarding its toxicity and carcinogenicity. Acetic acid exhibits favourable solubility characteristics for PCL. Because DMF has partial solubility parameters for PCL, using it as a co-solvent can change the chain entanglement, particle shape and chain-solvent interactions. Dimethylformamide can potentially be hepatotoxic, even though its toxicity varies depending on the patient's liver health, dosage and duration of exposure. Although they have been added to chloroform, formic and acetic acid solutions in several investigations to increase electrospinnability, methanol and ethanol are not PCL solvents.<sup>16-19</sup> The PCL degradation rate can be controlled by molecular weight, crystallinity or modifying the structure using hydrophilic polyethylene glycol (PEG), ceramics or the creation of copolymers with other polymers.<sup>14,20</sup>

Polycaprolactone has been approved by the FDA (Food and Drug Administration) and (Conformité Européenne [CE] marking) for use in a wide range of drug delivery and medical devices, but only a few have been marketed or translated into clinical research. In physiological conditions, PCL is degraded via hydrolysis of its ester bonds (such as in the human body). Polycaprolactone degrades in two stages: first, non-enzymatic hydrolytic cleavage of ester groups, and second, when the polymer is more highly crystalline and has a low molecular weight (less than 3000), the polymer is shown to undergo intracellular degradation, as evidenced by experiments of PCL fragments uptake in macrophage and giant cell phagosomes, as well as within fibroblasts.<sup>14,21</sup>

A promising material for biomedical applications can be generated by functionalising the fibrous structures of PCL using nanoparticles to give them new physical and chemical properties (improving the strength and endurance or enhancing antimicrobial and anti-inflammatory capabilities). It would also be necessary to add growth factors to obtain suitable properties for adequate tissue regeneration.<sup>22</sup>

Degradation studies of non-woven materials consisting of PCL nanofibers *in vitro* and *in vivo* revealed that electrospun PCL materials disintegrated considerably faster *in vivo* than *in vitro*, owing to enzymatic and hydrolytic degradation of PCL.<sup>23</sup> Polycaprolactone/ $\beta$ -Tri-calcium phosphate (TCP) composite scaffolds break down more quickly *in vivo* than PCL homopolymer scaffolds after six months.<sup>24</sup>

### *Antibacterial properties of PCL and its combinations*

Polycaprolactone alone does not possess antibacterial properties. This specific characteristic is crucial. Polycaprolactone is a form of polymer that may be broken down by a wide variety of bacteria. Polycaprolactone's qualities may be changed and improved by adding micro and nano-sized chemicals.<sup>25</sup> In addition to increasing susceptibility to infection, tissue damage caused by surgery or ingesting foreign materials also activates the host's defenses and encourages the generation of inflammatory mediators, which are boosted by bacterial activity and toxins.<sup>26</sup> Implants can be specifically employed in laryngology, as the sinus and nasal surgical fields are not entirely sterile. Numerous studies indicate the need for PCL changes to improve its bactericidal potency. Polycaprolactone itself has the potential to carry antimicrobial agents, and its alterations typically involve adding chemicals with well-known bactericidal properties, such as graphene, bioglass, copper, silver, zinc oxide or silver.<sup>27,28</sup> Low MBC (minimal bactericidal concentration; the minimum concentration needed to kill at least 99.9% of the bacteria cells) and minimal inhibitory concentration; the minimum concentration required to resist bacterial growth) values were indicators of the copolymers' high antibacterial activity.<sup>26</sup> Table 1 summarises the antibacterial effects of PCL combined with different materials in the form of composites.

### *Cytotoxicity studies of PCL and its associated compounds*

One of the methods for assessing and screening biological properties is the cytotoxicity test, which examines the effects of medical devices on cell growth, reproduction and morphology using tissue cells grown *in vitro*.<sup>54</sup> The ISO 10993-5 standard specifies three types of cytotoxicity tests: extract, direct and indirect contact (including agar overlay assay and filter diffusion). The extracted test is typically consistent with the results of animal toxicity testing and is useful for determining the toxicity of soluble components of medical devices. The direct contact assay is the most sensitive test for detecting even minimal cytotoxicity caused by medical devices. Molecular filtration and bulk filtering methods are both appropriate for assessing the biocompatibility of the hazardous components of small molecular-weight medical devices. The agar overlay assay is suitable for evaluating highly toxic medical devices.<sup>55,56</sup> Polycaprolactone's hydrophobic nature presents a challenge for tissue engineering, as it hinders cell adhesion. Therefore, various surface treatments have been explored to create a more conducive

**Table 1.** The antibacterial effect of PCL and composite of PCL and other components.

Composition	Effect	Reference
Polycaprolactone/ZnO membranes	Pure PCL membranes and fibre mats did not exhibit any antibacterial action against <i>Escherichia coli</i> and <i>Staphylococcus aureus</i> bacteria. However, the PCL membrane observed a statistically significant antibacterial effect against <i>E. coli</i> and <i>S. aureus</i> , including 5% and 6% ZnO nanoparticles.	(29)
Oligomeric/polycaprolactone	The ratio of PHMG (poly(hexamethylene guanidine) hydrochloride) to PCL affected the antibacterial action. The MIC and MBC for <i>E. coli</i> and <i>B. subtilis</i> were reduced when there was more PHMG present, demonstrating a relationship between the PHMG content and the antibacterial activity. MIC and MBC values for <i>E. coli</i> and <i>B. subtilis</i> were low for the pure PHMG oligomer.	(26)
The electrospun membrane of hyaluronic acid/polycaprolactone embedded with silver nanoparticles	The antibacterial activity of Ag in the HA/PCL + Ag NFM was demonstrated by examining the inhibition zones against bacterial strains; PCL and HA/PCL NFMs lacked any inhibition zones. <i>E. coli</i> and <i>S. aureus</i> were both susceptible to the antibacterial effects of HA/PCL + Ag NFMs. The findings also showed that HA/PCL + Ag NFMs had a weaker antibacterial effect against <i>S. aureus</i> than they did against <i>E. coli</i>	(30)
Silver octahedral nanoparticle/ Polycaprolactone nanocomposite	Ag-PCL scaffold reduced bacterial survival to 32.2% compared to conventional PCL scaffold. This survival inhibition was not as potent as that brought about by the same quantity of free Ag octahedral nanoparticles.	(31)
Polycaprolactone/quaternised chitosan blends	The findings demonstrated that polycaprolactone/chitosan did not significantly exceed plain PCL regarding antibacterial activity and that chitosan's antibacterial ability was constrained in blends. <i>Escherichia coli</i> and <i>Staphylococcus aureus</i> were inhibited by polycaprolactone/quaternised chitosan. Combinations showed 99.9% inhibition rates against both types of bacteria when the QCTS level was up to 20%.	(32)
Polycaprolactone/Copper oxide nanoparticle	No viable cell counts of MRSA (methicillin-resistant <i>Staphylococcus aureus</i> ) were found after 24 h of exposure to the active polymeric material at concentrations of 0.07% and 0.1% (w/w) CuONPs. While, the final MRSA growth for the 0.05% (w/w) CuONPs concentration was insufficient to have an inhibitory effect on the pathogenic strain	(33)
Polycaprolactone/cobalt-substituted hydroxyapatite composite	The bacterial colonies on the agar plates of the PCL-CoHA group significantly decreased compared to the control group	(34)

(Continued)

Table 1. (continued)

Composition	Effect	Reference
Polycaprolactone (PCL) films containing essential oils	The two bacteria employed in this investigation were tested for their susceptibilities to the compounds are <i>S. enterica</i> and <i>L. monocytogenes</i> . MICs and MBCs values for cinnamaldehyde addition to PCL were higher for both bacteria. <i>S. enterica</i> and <i>L. monocytogenes</i> , respectively, than of allyl isothiocyanate addition.	(35)
Electrospun polycaprolactone/polyethylene oxide/vancomycin nanofiber	For the samples, the VM-loaded nanofiber mat's (VMNF) antibacterial properties persisted for 14 days.	(36)
Nanohydroxyapatite/Polycaprolactone (nHA/PCL) electrospun membrane loaded with tetracycline hydrochloride (TCH)	Inhibition zones in <i>B. cereus</i> bacteria were larger than those in <i>E. coli</i> . This shows that the TCH medication has a greater impact on <i>B. cereus</i> than on <i>E. coli</i> . Electrospun nHA/PCL nanofibers loaded with 10% (w/w) TCH may effectively fight bacterial infection at the bone contact.	(37)
Polycaprolactone fibres loaded with Cefazolin	Without the addition of cefazolin, PCL fibres revealed that there were no inhibition zones around them. In light of this, it was determined that the neat PCL fibres had no bactericidal activity. Cefazolin-loaded PCL fibres for each system showed antibacterial action against microorganisms. For all samples, the amount of inhibition was greater against <i>S. aureus</i> than <i>E. coli</i> , as seen by a larger diameter of the inhibition zones.	(38)
Polycaprolactone/gelatin nanofibrous scaffolds coated with silver	The PCL and PCL gelatin nanofibrous scaffolds lacked antibacterial qualities against <i>B. cereus</i> or <i>E. coli</i> . Ag-coated PCL nanofibrous scaffold coated with the 1.25% AgNO <sub>3</sub> solution had a distinct inhibitory zone around Ag-coated nanofibrous stands for both bacteria. The sample only contained 0.8% Ag, which was insufficient to destroy the bacteria under investigation. However, increasing the Ag concentration to 4.2% revealed antibacterial capabilities.	(39)
PCL/Cu-BGNs	The findings show that adding Cu-BGN extracts to the medium suppressed the bacterial activity of <i>S. carnosus</i> and <i>E. coli</i> . Bacterial activity in the culture medium decreased by about 20% as Cu-BGNs incorporation increased, but it did not increase further as Cu release increased.	(27)

(Continued)

Table 1. (continued)

Composition	Effect	Reference
Electrospun mats composed of polycaprolactone fibres loaded with Zn	After 24 h of incubation, nanocomposite mats significantly inhibited <i>S. aureus</i> and <i>E. coli</i> development. Pure PCL-containing mats had negligible antibacterial effects. Both of the investigated bacterial strains had a 50% reduction in bacterial growth in the presence of nanocomposite mats. Still, the inhibition of <i>S. aureus</i> was slightly higher than that of <i>E. coli</i> . Increases in Zn concentration did not significantly improve the antibacterial activity of the mats.	(40)
Chitosan: PCL	It was discovered that PCL surfaces made using formic acid and acetone dissolution solvents had no antibacterial effects on <i>E. coli</i> . The antibacterial activity against <i>E. coli</i> was improved after mixing CHI at different ratios in PCL. It has been demonstrated that adding CHI to PCL improves its antibacterial activity significantly.	(41)
Poly ( $\epsilon$ -caprolactone) (PCL) fibre mats loaded with Peppermint Essential Oil as wound dressing.	Compared to PCL electrospun fibre mats, the bacterial viability on different concentrations of PEP loaded to PCL was reduced during the 48-h incubation. Additionally, a rise in PEP concentration improved the antibacterial activity.	(42)
Cinnamon/polycaprolactone	Various strains of <i>E. coli</i> , <i>S. aureus</i> , MRSA and <i>E. faecalis</i> were subjected to antibacterial tests. Cinnamon loading considerably increased the antibacterial activity of all evaluated fibres by lowering the bacterial cell count. The active cinnamon-containing fibres were compared to PCL alone, which has no innate antibacterial potential. Bacteria can sustain a population on the surface of PCL fibres since there are bacterial colonies there, which shows that the material's surface does not actively impede bacterial production.	(43)
Polycaprolactone/curcumin@zif-8 composite films	The antimicrobial effect of PCL/Cur@ZIF-8 composite films was studied by inhibiting the growth of bacteria, including <i>E. coli</i> and <i>S. aureus</i> , with cur and Cur@ZIF-8 loading ranging from 0% to 35%. The <i>E. coli</i> inhibition was approximately 99.9% when the nanoparticle loading was more than 15% (w/w). The survival rates of the <i>E. coli</i> group decreased as the content of Cur@ZIF-8 loading increased from 5% to 35%.	(44)
Polycaprolactone/Gelatin/Chrysin Scaffolds.	The majority of the microorganisms on the PCL were still alive, neither the PCL nor the scaffold's gelatin possessed any antibacterial properties. In contrast, the survival percentage of the bacterial population on PCL/Gel/Chrysin was extremely low. The rate of reduced bacterial growth in the PCL/Gel/Chrysin groups was considerably higher in the <i>E. faecalis</i> group compared to the <i>P. aeruginosa</i> group.	(45)

(Continued)



Table 1. (continued)

Composition	Effect	Reference
Essential oils loaded onto cellulose acetate/polycaprolactone wet-spun microfibers	The results demonstrated that the EO-modified microfibers were effective against the tested bacteria even at low concentrations, either by killing the bacteria more quickly or by more easily breaking their cytoplasmic membrane than ampicillin. The CLO-modified fibres from the EOs group were found to be the most efficient in terms of the amount immobilised. These findings suggest that improved antibacterial activity may be easily achieved in CA/PCL microfibers loaded with EOs, supporting the idea that these fibres could be used as scaffolding materials for the treatment of infections.	(46)
Thymol/SBA-15 Nanorods/PCL Electrospun Fibers	The ability of THY-loaded SBA-15 particles to kill bacteria like <i>S. aureus</i> was significantly lower than the free THY. When THY-loaded particles are incorporated into PCL fibres, the concentration of released active compounds rises, making it simpler to reach MIC and MBC values	(47)
Zn doped HMS/polycaprolactone Electrospun membranes	The antibacterial effect for hollow mesoporous silica nanospheres integrated into PCL membranes improved with the loading number of nanospheres in composite membranes. The addition of ClH to HMZS/P increased the antibacterial activity, indicating a synergistic antibacterial impact between the ClH and Zn <sup>2+</sup> .	(48)
Polycaprolactone/Thermally Reduced Graphene Oxide	The electroactive PCL/TrGO scaffolds showed a bactericidal effect. A reduction of 45% in the number of bacterial colonies adhering to polymer scaffolds was seen in the pure PCL scaffold (electrically non-conductive), but 100% of bacterial colonies were eliminated in the electroactive PCL/TrGO scaffolds.	(49)
Graphene (GNP)/PCL composite	PCL without additives exhibits only minimal antibacterial action against <i>S. aureus</i> . Antimicrobial efficacy is considerably improved by adding a little amount of graphene (0.5%), increasing it to 90% antibacterial efficiency.	(28)
PCL/Carbon Quantum DOTs	Film cast samples were tested for antibacterial efficacy using a variety of G+ and G-strains, specifically <i>S. aureus</i> , <i>E. coli</i> , <i>K. pneumoniae</i> and <i>L. monocytogenes</i> . The addition of hCQDs to PCL films enhanced their antibacterial effectiveness against all types of bacteria that were being employed. The antibacterial action was particularly notable in the cases of <i>S. aureus</i> , <i>E. coli</i> and <i>L. monocytogenes</i> . The effect was lessened in the case of <i>K. pneumoniae</i> .	(50)
Polycaprolactone Nanofibers Reinforced by Halloysite Nanotubes and Erythromycin	The HNT/ERY and PCL/HNT/ERY nanofibers showed substantial antibacterial activity; however, PCL and HNT/PCL were not antibacterially active, and no inhibitory zone was created.	(51)

(Continued)

**Table 1.** (continued)

Composition	Effect	Reference
Electrospun polycaprolactone membranes loaded with Rifampicin	Bacterial species ( <i>S. aureus</i> , <i>K. pneumoniae</i> , <i>A. baumannii</i> , <i>P. aeruginosa</i> and <i>E. coli</i> ) are severely inhibited from reproducing when PCL/Rif membranes are present. Against the investigated bacterial strains, PCL membranes show no antibacterial activity.	(52)
Silk fibroin/ polycaprolactone-polyvinyl alcohol composite film/ antibacterial drug/ microspheres for wound dressing materials	The outcomes demonstrated that the rate of bovine serum albumin (BSA) encapsulation by MSN-SF/CS drug-loaded microspheres was good for both biocompatibility and antibacterial activity	(53)

environment for cell growth and proliferation, such as treating PCL with different solutions to enhance its hydrophilicity and promote cell attachment to the polymer.<sup>57</sup> Prior attempts at using pure PCL could not provide the best possible mechanical strength and biocompatibility. Many studies have attempted to modify the PCL. Polycaprolactone scaffolds with a double protein coating have been shown to have better early cell adhesion, proliferation and colonisation.<sup>58</sup> When tested on isolated human tonsil-derived mesenchyme stem cells, Lee et al. demonstrated that a 3D PCL scaffold has osteoconduction. The cells rapidly underwent differentiation to become osteoblast-like cells with osteo-prompting properties.<sup>59</sup> Lin et al. designed a PCL composite membrane that contains 20 wt% of cobalt-substituted hydroxyapatite powder, significantly increased cell proliferation (over 90% after seven days of culture) was observed.<sup>34</sup> Ho et al. investigated the effects of Biodentine/PCL composite on human dental pulp cells. The bioactivity, proliferation and odontogenic differentiation of human dental pulp cells cultured on the composite exhibited a good apatite-forming ability and capability to support proliferation and differentiation.<sup>60</sup> The PCL / PEG hydrogel composite inhibits mineralisation and osteoblastic differentiation of cultured calvarial cells.<sup>61</sup> The PCL-Biosilicate composite showed adequate mechanical properties without increasing toxicity.<sup>62</sup> *In vitro* test of gelatin collagen (GC) and PCL with two different ratios (GC: PCL; 1:8 and 1:20) showed better cell proliferation on the composite with a lower collagen content when tested on adipose-derived stem cells.<sup>63</sup> Table 2 summarises the cytotoxicity effects of PCL and its associated composites.

### *Osseointegration of PCL composites*

Osseointegration is calculated using a sample of the implant and peri-implant bone that has been stained to determine the amount of peri-implant bone and bone-implant contact. Although accurate measurement is beneficial, long-term research cannot use it because of the invasive and damaging process. It is utilised in non-clinical research and testing. It is evaluated before, during and after surgery.<sup>67</sup> Due to PCL's hydrophobicity and lack of functional groups that encourage cell growth and proliferation, cellular interactions are restricted. Modifications are required to improve the PCL's cellular compatibility and capacity for bone repair. Protein adsorption, necessary for cell identification and attachment, decreases at very low contact angles due to an increased water intake. However, low surface energy and very high contact angle result in poor cell conductivity and protein denaturation. Arginine-glycine-aspartic acid-PCL composite demonstrated smoother surfaces and early bone deposition onto composite surfaces.<sup>68,69</sup> *In vivo* blending of 1% Sr<sup>2+</sup> with PCL greatly accelerated bone tissue regeneration without causing localised irritation.<sup>70</sup> Combining calcium lactate and cellulose acetate solutions with a PCL nanofibrous scaffold significantly improves the composite fibre's bio-physio-chemical characteristics.<sup>71</sup> When PCL is functionalised with polydopamine and rhBMP2, the surface wettability, cell proliferation and osteogenic potential are improved.<sup>72</sup> Compared to pure PCL, hydroxyl-functionalised PCL exhibited 70% porosity, improved cell adhesion, higher metabolic activity and osteogenic potential.<sup>73</sup> According to Spalthoff,<sup>74</sup> PCL-TCP composite indicated that a significant portion of the composite material had deteriorated and been replaced by vital bone.

**Table 2.** Summary of cytotoxicity effect of PCL and PCL blended compound.

Cell line	Composition of tested groups	Effect	References
hPDLSC cultures	PCL of different concentrations (14, 16 and 20 wt.% in glacial acetic acid)	the evaluated scaffold did not significantly affect the viability of the cells and had no detrimental or inhibiting effects on the cells' ability to develop.	(64)
Osteoblast-like MG-63 cells.	PCL/PMMA, with different concentrations (10/0, 7/3, 5/5 and 3/7)	the 7/3 PCL/PMMA scaffold showed higher cell proliferation than another concentration scaffold	(65)
human dermal fibroblast cells.	Gentamicin sulphate was added to PCL-Tri calcium phosphate in amounts of 5wt%, 15wt% and 25wt%.	Cell viability was considerably lower in the PCL-TCP-2.5% Gentamicin group at the 48 h and 72 h time points than in the other groups, showing that the GS dosage had a negative impact on cell viability.	(66)
Adult Goat Fibroblast cell.	PCL/ZnO (with varying ZnO concentrations, ranging from 0.1 to 0.9 weight percent to 1-6 weight percent)	The highest cell proliferation was observed in membranes containing 1% ZnO nanoparticle concentration, while the lowest cell proliferation was observed in those possessing a 6% concentration. But none of the membranes were toxic to cells because they all had more than 100% viability.	(29)
L929 (CCL-1, ATCC) cell line	<ul style="list-style-type: none"> <li>• PCL</li> <li>• poly(hexamethylene guanidine) PHMG</li> <li>• poly(hexamethylene guanidine) PHMG: PCL copolymer.</li> </ul>	PHMG shows cytotoxicity effect, the copolymers less cytotoxic.	(26)
human Hs68 fibroblasts	<ul style="list-style-type: none"> <li>• PCL nanofibers membrane</li> <li>• HA/PCL nanofibers membrane</li> <li>• HA/PCL + Ag nanofibers membrane</li> </ul>	There were significantly fewer viable cells on the HA/PCL + Ag NFM than on the HA/PCL NFMs, which were even less than the PCL NFMs. It has been found that Ag nanoparticles contained in polymeric NFMs inhibit fibroblast growth and cell adhesion.	(30)
HSF cells	Polycaprolactone (PCL) and PCL/gelatin (Ge) (70:30) Nanofibrous scaffolds were coated with silver (Ag) in different concentrations (1.25, 2.5, 5 and 10%)	Cells were unaffected by Ag-coated PCL and PCL/Ge (70:30) nanofibrous scaffolds.	(39)

(Continued)

Table 2. (continued)

Cell line	Composition of tested groups	Effect	References
primary human dermal fibroblast (HDF)	Zinc oxide nanoparticles were added to PCL in different concentrations (9, 12, 15 and 25 wt.%).	There was no evidence of toxicity.	(40)
NHDF cells	<ul style="list-style-type: none"> <li>PCL fibre mats.</li> <li>PCL: 1.5 v/v% peppermint essential oil fibre mats.</li> <li>PCL: 3 v/v% peppermint essential oil fibre mats.</li> <li>PCL: 6 v/v% peppermint essential oil fibre mats.</li> </ul>	PCL electrospun fibre mats that were loaded with PEP had no toxic effects on NHDF cells.	(42)
HFF-1 cells	<ul style="list-style-type: none"> <li>PCL</li> <li>0.05% Cuppor Oxide Nanoparticles PCL</li> <li>0.07% Cuppor Oxide Nanoparticles, PCL</li> <li>0.1% Cuppor Oxide Nanoparticles,</li> </ul>	fibroblast cells showed an average cell viability of more than 80% for all groups except PCL + 0.05% CuONPs. The normal fibroblast morphology of HFF-1 cells treated with PCL + 0.07% CuONPs film.	(33)
Commercial hBM-SCs	<ul style="list-style-type: none"> <li>PCL</li> <li>PCL + 5% wt TrGO.</li> <li>PCL + 10% wt. TrGO</li> <li>PCL + 15% wt. TrGO</li> <li>PCL + 20% wt TrGO</li> </ul>	Scaffold does not produce any cytotoxic effect on human cells but also generate greater cell viability	(49)
L929 mouse fibroblast cell line	<ul style="list-style-type: none"> <li>15% PCL</li> <li>15% PCL + 250 mg/mL cinnamon.</li> <li>15% PCL + 375 mg/mL cinnamon.</li> <li>15% PCL + 500 mg/mL cinnamon.</li> </ul>	Each fibre sample kept its viability above the cytotoxic threshold by a substantial margin.	(43)

Compared to the pure PCL, cell growth is noticeably greater in composites, including those made of recombinant PCL/SF (Silk Fibroin) composite, spider silk protein/PCL/gelatin, PCL/chitosan composite and PCL/biphasic calcium phosphate hybrid composite.<sup>75-77</sup>

Increased cell proliferation is made possible by adding HA to the PCL/SF composite scaffold. At the same time, collagen-I synthesis is lowered, and osteoinductivity is highly favoured by adding bone morphogenetic protein 4-expressing bone marrow stromal cells.<sup>78,79</sup> Table 3 lists the effects of pure and blended PCL when implanted inside a live animal.

## Barium titanate

Barium titanate ( $\text{BaTiO}_3$ ) is a polycrystalline ceramic material with ferroelectricity properties with perovskite structure ( $\text{ABO}_3$ ) (Figure 1). The unique features and widespread use in a variety of devices, ferroelectrics are gaining popularity.<sup>87,88</sup> The bulk physical characteristics and crystal structure of  $\text{BaTiO}_3$  have been extensively studied since Wul and Goldman discovered  $\text{BaTiO}_3$  ferroelectricity in 1945.<sup>89</sup>

The  $\text{BaTiO}_3$  exhibits four crystal phases in bulk: cubic, tetragonal, orthorhombic and rhombohedral. At high temperatures ( $T > 120^\circ\text{C}$ ), it has the conventional perovskite structure (i.e. cubic phase), in which  $\text{Ba}^{2+}$  and  $\text{O}^{2-}$  ions form the FCC lattice ( $\text{Ba}^{2+}$  at the corners and  $\text{O}^{2-}$  in the center of each face of the lattice). At the same time, the smaller  $\text{Ti}^{4+}$  cation occupies the octahedral interstitial spaces, forming  $[\text{TiO}_6]$  in the FCC array.<sup>90,91</sup>

The cubic phase structure of  $\text{BaTiO}_3$  is very symmetric, with cation and anion centers coinciding, resulting in no polarisation in the crystal structure and, therefore, no ferroelectricity (i.e. paraelectric). Upon reducing the temperature to less than  $120^\circ\text{C}$ , the cubic symmetric structure becomes non-symmetric due to a deviation of the cation center from the anion center, leading to net spontaneous polarisation in the crystal structure and transition from paraelectric to ferroelectric phase, exhibiting a tetragonal structure. Further cooling between  $-5^\circ\text{C}$  and  $-90^\circ\text{C}$  leads to the conversion to the orthorhombic phase, which can be considered the elongation of the cubic unit cell in the face diagonal direction. Finally, at  $T < -90^\circ\text{C}$ , the rhombohedral phase occurs, which represents the elongation of the cubic unit cell along with the body diagonal direction. Non-symmetry in the crystal structure results from distortions along with these directions, with the deviation of the cation center from the anion center, resulting in ferroelectric phases with net spontaneous polarisation (Figure 2).<sup>89,91</sup>

Barium titanate ( $\text{BaTiO}_3$ ) piezoelectric ceramic is often used to stimulate bone regeneration by mimicking natural bone stress-generated potentials, which produce micro-electric currents and enhance calcium salt deposition at the bone defect site. The piezoelectric polarisation stimuli generated by  $\text{BaTiO}_3$  can modify bone development, shaping and reconstructing the tissue as native bone undergoes deformation.<sup>92</sup>

The domain in piezoelectric ceramic materials refers to many unit structures having the same polarisation orientation. Each part has its polarisation direction, randomly orientated to keep the material's net polarisation at zero without an external electric field (EF).<sup>93</sup> A strong external voltage applied at a high temperature aligns the domains parallel to the direction of the applied EF.<sup>94</sup>

**Table 3.** Summary of osseointegration effect of pure PCL and blended PCL

PCL composite	Effect	Reference
PCL/HAp HAp (0–50% w/w of PCL).	When compared to pure PCL counterparts, all of the PCL/HAp scaffolding implants showed a greater amount of new bone development.	(80)
3D Printed and micropatterned polycaprolactone scaffolds	In this study, the scaffolds with coupled hierarchical mesoscale and microscale characteristics can align cells <i>in vivo</i> for oral tissue healing, with the potential to enhance additional bone-ligament complexes' regenerative responses.	(81)
Polycaprolactone Nanocomposite	The nanocomposite PCL group's healing region showed production of primary bone and granulation tissue on the fifteenth day of healing, resulting in an incomplete organic bone matrix with hemorrhages. The healing area in the nanocomposite PCL group also demonstrated that woven bones were being created on the 30th day of healing. The nanocomposite PCL group reported that the defect had been filled with lamellar bone on day 45 of the healing phase.	(82)
Electrospun polydioxanone (PDO)/ polycaprolactone (PCL) scaffold.	Diffuse regions of foreign body giant cells were visible in the electrospun scaffold zone. The tissue incorporated into the electrospun scaffolds was supported by a network of blood vessels. The patch scaffold included the neovascularisation that was noticed. Neutrophils that can be recognised by H&E staining based on their distinctive morphology were not found.	(83)
Poly-ε-Caprolactone Scaffolds	Fibroconnective tissue completely encased each scaffold. No inflammatory symptoms or unfavourable tissue reactions were noticed. The scaffold was surrounded by fatty and fibrous tissue, as seen in HE-stained slices. Giant multinucleated histiocytes encircled the scaffold's fibres.	(84)
PCL/PMMA	New bone tissue and undifferentiated cells were seen around the PCL/PMMA scaffold.	(65)
PLA/PCL/metformin-loaded gelatin nanocarriers	The <i>in vivo</i> results showed that MET/GNs-PLA/PCL enhanced bone ingrowth, angiogenesis and defect reconstruction.	(85)
polycaprolactone/gelatin nanofibrous nerve guided conduit/platelet-rich plasma/citicoline for peripheral nerve regeneration.	The implantation of PCL/Gel/PRP/Citi NGC caused regeneration of nerve tissue, with recovery of motor and sensory functions, according to <i>in vivo</i> investigations on sciatic nerve injury in rats.	(86)
PCL scaffold PCL dissolved in acetone solution (17 wt-%)	The <i>in vivo</i> results showed that the electrospun meshes had a clear biointegration.	(23)

The piezoelectric action of BaTiO<sub>3</sub> was discovered to enhance osteoblast development. It should be highlighted that most prior research used bulk BT materials. Bone tissue regeneration occurs mainly at the implant-tissue interface during the first four months of the healing period for hard tissue replacement materials. As a result, tiny micro-scale BT coatings coated on artificial metal (Ti or Zr alloys) implants will be more favourable. The latter could provide protective coatings for implants while also achieving electroactive performance. The solid-state reaction, sol-gel technique and physical vapor deposition are now used to make BT coatings or films.<sup>95</sup>

Barium titanate demonstrates good biocompatibility and the ability to develop a strong interfacial connection with the surrounding bone. The biocompatibility of BT in its nanoparticle form has been confirmed through various animal studies, which revealed no signs of a foreign body or inflammatory reactions at the implant-tissue interface. These results indicate that BT has excellent systemic non-toxicity, paving the way for developing new biomedical applications based on BaTiO<sub>3</sub>-based materials.<sup>88</sup>

On CpTi, BaTiO<sub>3</sub>/TiO<sub>2</sub> double layers' electrolytic deposition has been successfully conducted to examine its properties. Nanocrystalline BaTiO<sub>3</sub>/TiO<sub>2</sub> specimens have a smaller grain size and a denser structure, which improves corrosion resistance and bioactivity. Furthermore, it was demonstrated that the piezoelectric ceramic (BaTiO<sub>3</sub>/TiO<sub>2</sub>) double layers exhibit higher biocompatibility and strong substrate adhesion.<sup>96</sup>

Coatings of HA/BT/CS nanocomposites with various HA/BT ratios were placed on 316L stainless steel substrates. The hardness diagram and impedance spectra data demonstrated that adding BT to the implant coating increased the coating's corrosion resistance. The samples' SEM and AFM data also revealed apatite forms on the implants' surface after 28 days of immersion in the SBF solution, suggesting the coating's bioactivity.<sup>97</sup>

### ***Antibacterial properties of BT***

The majority of bioimplant treatments fails and requires revision surgery due to bacterial infections.<sup>98</sup> A biofilm is initially produced during the development and spread of bacterial contamination. Gram-positive (GP) and Gram-negative (GN) bacteria can cause infections. GP bacteria comprise *Staphylococcus aureus* and Streptococcus species, while *Pseudomonas aeruginosa*, *Enterococcus species* and *Enterobacter aerogens* are examples of GN bacteria.<sup>99</sup> The treatment of bone infections has made considerable use of antibiotic applications. Nevertheless, an appropriate antimicrobial stewardship program is needed for complete infection control. According to this viewpoint, an antibacterial agent would treat a chronic infection for up to four weeks.<sup>100</sup>

Numerous strategies have been used to completely eradicate infections, including altering the composition of implants, altering the level of roughness of the coating and applying external factors such as electric and magnetic stimulation. Based on the substance used, the seriousness of the infection, and the patient's reaction to therapy, antibiotics may be given to a patient for a short or long period of time.<sup>101</sup> Using a polarised EF has a huge advantage since it works as a microbiological inhibitor due to the harmful effects of using antibacterial drugs in biomaterials simultaneously on the human body. Bacterial negatively charged cells typically develop that charge on their surface due to the ionisation of functional groups such as phosphate, amino, hydroxyl and carboxyl



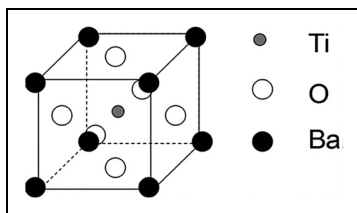


**Figure 1.** Crystalline structure of BT material.<sup>67</sup>

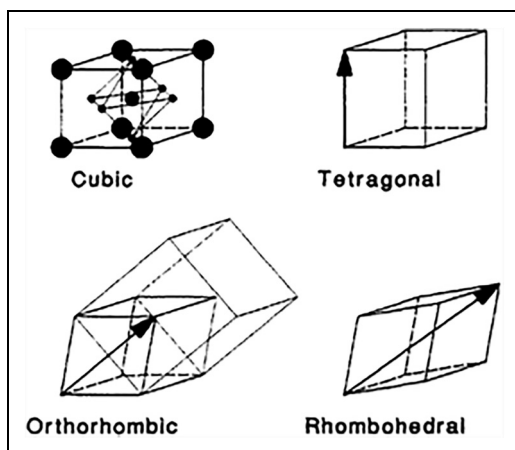


**Figure 2.** A schematic representation of the four different crystalline structures of  $\text{BaTiO}_3$ .<sup>89</sup>

groups. Exogenous agents, including electric and magnetic fields, have recently been applied to suppress bacterial populations.

In contrast, the human body's electrical charge maintains the control of cell action. To manage bacterial activity without endangering human health, it is important to thoroughly explore the stimuli created by an intrinsic electrical charge in treating bacterial infections.<sup>102,103</sup> Both internal and external factors influence any material's biological reaction. Their size and shape significantly influence the internalisation of nanoparticles. Different forms of endocytosis, such as phagocytosis, pinocytosis, receptor-mediated cytosin, etc., are possible. Additionally, the surface charge of the nanoparticles, their structural composition and the position of ions in the lattice structure all affect how cells behave, which significantly impacts how biologically responsive the nanomaterials are under investigation.<sup>104,105</sup>

Reactive oxygen species (ROS), produced when high-intensity laser beams come into contact with metal-based nanoparticles, might be used to generate new antibacterial substances. Shah et al. assessed the antibacterial activity of  $\text{BaTiO}_3$  nanoparticles (approximately 100 nm) against human pathogenic bacteria. Through this work,  $\text{BaTiO}_3$  NPs have shown a dose-dependent substantial reduction in gram-positive and gram-negative

bacterial growth and strongly affected biofilm formation against clinical isolates of *P. aeruginosa* and *S. aureus*.<sup>106</sup>

Sasikumar et al. demonstrated the antimicrobial activity of hydrothermally synthesised cubic-shaped BaTiO<sub>3</sub> NPs. At very low doses, these NPs have shown antimicrobial activity against *C. albicans* and various multidrug-resistant pathogens. These antimicrobial activities result from decreased ergosterol biosynthesis in *C. albicans*. Incorporating BaTiO<sub>3</sub> NPs in the PLA fibres shows both bactericidal and bacteriostatic properties. They showed a dose-dependent response to the growth of *Staphylococcus epidermidis*.<sup>107,108</sup> Table 4 lists the antibacterial application of BT and its composite materials.

### Cytotoxicity studies of BT

The breakdown of BaTiO<sub>3</sub> biomaterial resulted in the release of Ba<sup>2+</sup>, a distinctive element in the human body, but is present in trace amounts in natural bone minerals (2.54 ± 0.16 ppb). This element may be cytotoxic.<sup>112,113</sup> Although investigation into the underlying processes governing the toxicity of BaTiO<sub>3</sub> is ongoing, oxidative damage might be due to the overproduction of ROS that have been connected to these mechanisms.<sup>114,115</sup>

In one investigation, human lung cancer cells (A549) with a dosage rate of 50 g/mL of BaTiO<sub>3</sub> showed substantial oxidative stress. This concentration range of BaTiO<sub>3</sub> was emphasised to exhibit a decrease in cell viability.<sup>114</sup> Similar findings were also reported by Staedler et al. (50 g/mL) of BaTiO<sub>3</sub> was tested for its time-dependent cytotoxicity on A549 cells, with cell survival rates of almost 91%, 84% and 81% following exposures of 24 h, 48 h and 74 h, respectively.<sup>116</sup>

The type of cell lines and the duration of exposure significantly impact the dose to be provided and the cell survival rate. In this work, the cytotoxicity of BaTiO<sub>3</sub> NPs (50 g/mL) was assessed on adenosquamous carcinoma cell line (HTB-178), non-tumoural BEAS-2B cells and lung squamous carcinoma cell line (HTB-182). Interestingly, HTB-178 exhibited the lowest percentage of cell survival at about 74% after a 72-h exposure.<sup>117</sup>

Similar results were observed by Bonacino et al., where a range of harmonic nanoparticles, including BaTiO<sub>3</sub>, were investigated for cytotoxicity effect on A549, BEAS-2B, HTB-178 and HTB-182 cells for an exposure time of (5 and 24) h.<sup>118</sup> Most cell lines showed a 20–30% reduction in cell viability at a 50 g/mL dosage rate of BaTiO<sub>3</sub>. Genchi et al. reported a slight influence on the percentage of viable cells when studying the response of human neuroblastoma cells (SH-SY5Y) towards P(VDF-TrFE)/ BaTiO<sub>3</sub> NPs films.<sup>119</sup> There is still much to discover about the precise processes behind cell responses to piezoelectric stimulation. The size of the BaTiO<sub>3</sub>, the mechanism of functionalisation and the kind of cells under examination are only a few variables that may impact their internalisation, followed route and associated cellular expressions.<sup>120</sup> Table 5 summarises BT's cytotoxic effect in pure and mixed form.

### Osseointegration evaluation of BT

The analysis of the BT implants through histology provided some valuable insights regarding the tissues grown in the pores, its high compatibility with hard tissues, and

**Table 4.** Summary of antibacterial application of barium titanate and its blended materials.

Barium titanate and barium titanate blend materials	Effect	Reference
Barium Titanate(BT)/Hydroxyapatite(HA) <ul style="list-style-type: none"> <li>• 60 wt% BT + 40 wt% HA</li> <li>• 40 wt% BT + 60 wt% HA</li> </ul>	The percentage of bacteria ( <i>S. aureus</i> , <i>E. coli</i> and <i>P. aeruginosa</i> ) that were reduced after being cultured was assessed, and it was discovered that the polarised 60BT + 40HA sample had the greatest impact on the number of bacteria that were reduced, followed by the 40BT + 60HA sample.	(103)
Barium Titanate Nano-particles <ul style="list-style-type: none"> <li>• BaTiO<sub>3</sub> NPs</li> </ul>	BaTiO <sub>3</sub> NPs exhibited high antibacterial activity against <i>S. aureus</i> and good activity against <i>P. aeruginosa</i> . The BaTiO <sub>3</sub> NPs exhibit excellent antibiofilm properties in addition to having a positive antibacterial effect.	(106)
Nano BaTiO <sub>3</sub> is prepared by surfactant (Hexadecyltrimethylammonium bromide, CTAB) <ul style="list-style-type: none"> <li>• concentration of CTAB (5, 10 or 15 mM) were added to BT.</li> </ul>	When compared to nanoparticles made without a surfactant, 15-CBT Nano BaTiO <sub>3</sub> exhibits higher antibacterial activity against all pathogens ( <i>C. albicans</i> , <i>E. coli</i> , <i>S. flexneri</i> , <i>V. cholerae</i> and <i>K. pneumonia</i> ).	(107)
Polyvinylidene fluoride (PVDF)/barium titanate (BaTiO <sub>3</sub> )/Ag composites <ul style="list-style-type: none"> <li>• PVDF/Ag-pBT scaffold</li> <li>• PVDF/pBT scaffold</li> </ul>	The PVDF/Ag-pBT scaffold could effectively inhibit <i>E. coli</i> growth. On the PVDF/pBT scaffold, a low bacterial inhabitation zone was observed.	(109)
PMMA/ceramic composites <ul style="list-style-type: none"> <li>• PMMA /aluminum nitride (AlN)</li> <li>• PMMA /barium titanate (BaTiO<sub>3</sub>)</li> <li>• PMMA /rutile (TiO<sub>2</sub>)</li> </ul>	When compared to the pure reference, only aluminum nitride or barium titanate PMMA had significant antibacterial activity (against <i>E. coli</i> ).	(110)
PLA-BaTiO <sub>3</sub> Composite Fibers <ul style="list-style-type: none"> <li>• PLA</li> <li>• PLA + 5%BT</li> <li>• PLA + 10%BT</li> <li>• PLA + 15%BT</li> </ul>	The quantity of surviving bacteria ( <i>Staphylococcus epidermidis</i> ) and their distribution decreased as the concentration of BT was increased in contrast to the PLA matrix, indicating a possible impact of the inorganic filler.	(108)
Polyvinyl-Siloxane / Barium Titanate Scaffolds <ul style="list-style-type: none"> <li>• Polyvinyl-Siloxane +35% Barium Titanate</li> <li>• Polyvinyl-Siloxane +65% Barium Titanate</li> </ul>	The composite demonstrated a beneficial effect against <i>Staphylococcus epidermidis</i> ,	(111)

**Table 5.** Summary of the cytotoxic effect of barium titanate in pure and mixed form.

Cell line used	Composite	Effect	References
SH-SY5Y cells	Glycol-chitosan and Doxorubicin / Barium Titanate Complexes for Cancer Therapy <ul style="list-style-type: none"> <li>• 0, 5, 10, 20, 50 and 100 µg/ml of GC-BTNPs.</li> </ul>	The result of this study shown that the treatment of cell cultures with high doses of BTNPs (100 g/ml) had no negative effects.	(121)
Murine fibroblast cells (L929 cell)	Porous barium titanate/hydroxyapatite composites bone tissue engineering <ul style="list-style-type: none"> <li>• HA50/BT50</li> <li>• HA30/BT70</li> <li>• HA10/BT90</li> </ul>	The composite of 30HA/70BT that had the maximum cell viability up to 201% was produced. This proved that the HA/BT composites with all of the HA/BT contents in volume percentage had good biocompatibility and did not have any cytotoxic effects on the L929 cells.	(122)
Human bone marrow mesenchymal stem cells.	Barium titanate/akermanite composite for bone defect recovery <ul style="list-style-type: none"> <li>• BT90/nAK10</li> <li>• BT75/nAK25</li> <li>• BT60/nAK40</li> </ul>	The results of the MTT experiment showed that the produced scaffolds had no cytotoxic effects. The cells in contact with the BT60/nAK40 scaffold have a higher viability time than the cells in contact with the other two scaffolds.	(123)
MC3T3-E1 murine pre-osteoblasts	Loading of Barium Titanate on the Collagen/Hydroxiapatite Composite Scaffolds <ul style="list-style-type: none"> <li>• Collagen-hydroxyapatite (Coll-HA) scaffold</li> <li>• Collagen-hydroxyapatite-barium titanate (Coll-HA/BT).</li> </ul>	The number of metabolically active viable cells increased more noticeably when BT was present in the Coll-HA scaffolds.	(124)
MG-63 cell line.	Electrodeposition Coating of Barium Titanate on Ti6Al4V	Cell seeding also demonstrated strong surface attachment, although MTT assay results in a lack of proliferation, which may be caused by ion leaching. The results thus demonstrate the BTO coating's suitability for use as an implant coating for <i>in vivo</i> applications.	(125)

(Continued)

Table 5. (continued)

Cell line used	Composite	Effect	References
Third-generation neonatal Sprague-Dowley rat osteoblasts	Graphene/barium titanate/ magnesium phosphate bio-piezoelectric composites	The results showed that the synthetic composites were biocompatible and had no negative impacts on the cells.	(126)
human dermal fibroblasts (HDF)	PLA-BaTiO <sub>3</sub> Composite Fibers	There were no discernible differences between composites and the PLA matrix; nevertheless, the high hydrophobicity of the fibres, reduced fibroblast attachment. Cell viability was best in the PLA 5% BT.	(108)
Human lung cancer cells (A549) and non-cancerous human lung fibroblasts (IMR-90)	Barium Titanate (BaTiO <sub>3</sub> ) Nanoparticles through Oxidative Stress <ul style="list-style-type: none"> <li>different concentrations of Barium Titanate NPs (5–200 µg/mL)</li> </ul>	The results indicate that BT NPs cause cytotoxicity in human lung carcinoma (A549) cells that is dose- and time-dependent. Cytotoxicity, pro-oxidant generation and antioxidant depletion caused by BT NPs were all significantly reduced by co-exposure to an antioxidant (N-acetyl-cysteine), indicating that oxidative stress was a mediator of BT NP-induced toxicity.	(114)
human osteoblast-like Saos-2 cells	Beta-Titanium Alloy coated with BaTiO <sub>3</sub>	With a cell viability of over 98% and other well-preserved cell activities, BaTiO <sub>3</sub> film demonstrated that this coating was not cytotoxic.	(127)

the frequent occurrence of direct bone apposition to the implant surface. Short-term studies indicated an increase in actively depositing osteoblasts near the implant. In contrast, long-term studies showed a slight reduction in the number of osteoblasts and the transformation of trabecular bone into compact bone, a typical response of healthy bone to a biocompatible implant. A comparison between a PTFE membrane and a composite of poly (vinylidene fluoride trifluoroethylene), P(VDF-TrFE) and BT ( $\text{BaTiO}_3$ ) (P(VDF-TrFE)/BT) revealed through histomorphometric and gene expression analyses that the latter promotes new bone formation when implanted in rat calvarial bone defects. Therefore, this composite could replace the current biomaterials used in GBR treatments.<sup>128</sup> Fan et al.<sup>92</sup> reported that electroactive BT-coated titanium scaffold conditions significantly accelerated osteogenesis and osseointegration six and twelve weeks after implantation in extensive segmental bone defects in the rabbits' radius, according to histomorphology and the peak pull-out load.

The BT/PLA (barium titanate/poly lactic acid) composite film, created using the solution casting process, has strong biocompatibility and piezoelectric capabilities. It had a good osteogenic effect in an *in vivo* study of rat cranial defects with the ability to direct bone tissue and support bone tissue regeneration.<sup>129</sup>

## Barium titanate-PCL (BT-PCL) composite

$\text{BaTiO}_3$  has well-known piezoelectric and biocompatible characteristics. Piezoelectricity has been demonstrated to be effective in biological processes, particularly those strongly related to bone activity. The bones' ability to convert functional stress into the electrical stimulation required for regrowth and repair has been well demonstrated, and it's essential to mention that the drawbacks of high brittleness and strong resistance to deterioration accompany the high piezoelectric coefficient of piezoelectric ceramic. The biopolymers are biodegradable but have no piezoelectric or mechanical strength, limiting their usefulness. With the help of the piezoelectric property, the mechanical strength of the piezoelectric composite of biopolymer and piezoelectric ceramic can be increased, and the signal of the cells may be recognised. PCL is a biodegradable polymer widely employed in implantable biomaterials.<sup>130,131</sup> The PCL-BT composites'  $d_{33}$  piezoelectric coefficient increased as the amount of  $\text{BaTiO}_3$  increased. Significantly, as compared to the unmodified PCL specimen, the  $\text{BaTiO}_3$  inclusion up to 25 vol.% steadily improved the piezoelectric response to 1.2 pC/N; more specifically, the PCL-45BT and PCL-65BT specimens showed an improvement in the piezoelectric response of 2.4 and 2.6 pC/N, respectively. Similar findings about  $\text{BaTiO}_3$  were also noted in some previous works.<sup>122,132</sup> For example, Liu et al.<sup>82</sup> found that when the  $\text{BaTiO}_3$  incorporation extent rose over 35 vol.% in the PCL matrix, there was a significant increase in the  $d_{33}$  values, up to 3.9 pC/N. The dense dispersion of  $\text{BaTiO}_3$  particles in the PCL-45BT and PCL-65BT specimens is the cause of the sharp increase in the  $d_{33}$  coefficient. A stronger electroactive response is produced due to the network of interacting  $\text{BaTiO}_3$  particles creating an EF through tight spacing. The PCL-25BT specimens, on the other hand, had less electroactive reactions due to the  $\text{BaTiO}_3$  particles' sparse distribution.

Zhang et al.'s investigation of porous HA- $\text{BaTiO}_3$  composites revealed  $d_{33}$  values ranging from 0.3 to 2.8 pC/N.<sup>122</sup> The polarised HA- $\text{BaTiO}_3$  piezoelectric ceramics

with a BaTiO<sub>3</sub> concentration ranging from 80% to 100% have d<sub>33</sub> values that Tang et al.<sup>132</sup> observed in the 1.3–6.8 pC/N range. High-volume BaTiO<sub>3</sub> contents are required in the HA-BaTiO<sub>3</sub> composites since some with less than 80 vol.% BaTiO<sub>3</sub> did not show any piezoelectric action.<sup>133</sup>

Conversely, due to the tight packing density of the piezoelectric BaTiO<sub>3</sub> particles in a sintered sample, specific bulk-sintered HA-BaTiO<sub>3</sub> composites showed exceptionally high d<sub>33</sub> values (>50 pC/N).<sup>134</sup> BaTiO<sub>3</sub> particles are not closely packed in a polymer matrix, which prevents polymer–ceramic composites like PCL-BT from ever displaying such a strong piezoelectric response. A strong scaffold-mediated piezoelectric response for bone regeneration is unnecessary because the bone has a piezoelectric response between 0.7 and 2.3 pC/N. Compared to HA-BaTiO<sub>3</sub> composites made using various traditional methods, the d<sub>33</sub> values of the 3D-printed PCL-BT composites were comparable to the piezoelectric response of bone. Therefore, the PCL-BaTiO<sub>3</sub> composites' noted piezoelectric response emphasises its enormous potential for osteogenesis and bone remodelling, accelerating orthopedic and dental applications.<sup>131,135</sup>

Liu et al. prepare the PCL/BT composite using a solution blending technique. Particles of PCL and BT were dissolved in tetrahydrofuran at different ratios (PCL with 5%, 10%, 15%, 20%, 25% BT). The composite flocs were precipitated by adding the PCL and BT liquid mixture to the ethanol. No cytotoxicity was observed when the composite was tested against the osteoblast line MG63 in DMEM.<sup>131</sup>

Composite scaffolds for skin regeneration composed of PCL 3D-printed scaffolds containing 500 mg/ml of BT piezoelectric nanoparticles were prepared. With a distance of 11 cm, a flow rate of 1.5 ml/h and a voltage of 10 kV, BT and PCL solutions were electrospun. Cell proliferation capacity and cellular responsiveness to the piezoelectric substrates were studied *in vitro*. The proliferation of NIH 3T3 fibroblasts was analysed while cultivated on PCL and PCL/BTNP scaffolds. When electrospinning is used with 3D-Bioplotting, a scaffold with multi-scale porosity is produced. *In vitro* cell viability analyses on this piezoelectric composite scaffold have shown that it provides a healthy environment for 3T3 and SaOS-2 cell adhesion, growth and proliferation. Compared to nanofibrous mats and 3D-printed scaffolds without fibres, the number of viable cells on composites is large.<sup>136</sup> Piezoelectric BT nanoparticles have been incorporated into the framework to mimic the responsiveness of the wound dressing. Recently, some research teams have started looking into how an EF affects the healing process of wounds. These investigations show that an electric stimulus, which mimics the physiologic endogenous EFs that arise with an injury, can efficiently stimulate skin regeneration.<sup>88</sup>

Successfully created PCL-BT 3D-printable filaments that can be used for maxillofacial, cranial and dental applications in addition to orthopedic ones. Activating calcium-sensing receptors or boosting Ca<sup>2+</sup> influx into osteoblast cells are two ways Ca<sup>2+</sup> regulates osteoblast development. As a result, the electrical stimulation (caused by the piezoelectric effect) from the PCL-BT scaffolds activated the calcium-sensing receptors, started the electrically sensitive Ca<sup>2+</sup> signal transduction and increased the Ca<sup>2+</sup> influx into MC3T3-E1 cells.<sup>14,130</sup> Ibrahim et al.<sup>137</sup> explained that adding 36% of BT to 18% of PCL improved the wettability performance of the composite coating on CpTi and Ti3Nb13Zr alloys. Improving the wettability property increases the performance of the composite in osseointegration.

This review has several limitations: 1. The methods of fabricating scaffolds or coatings or the possibility of these methods affecting biological properties were not discussed. 2. biodegradability, bioresorption, biomineralisation and the factors affecting them were not evaluated. 3. No specific criteria were specified when collecting information from different references. 4. The effect of piezoelectricity on biological properties has not been discussed. These limitations will be the main topics of investigation in future research work.

## **Challenges and future perspective of PCL, BT and their composites**

BT-PCL composites exhibit significant potential for utilisation in various biomedical applications. PCL-BT composites offer numerous benefits, including cost-effectiveness and the convenience and adjustability of manufacturing processes. The PCL-BT composites exhibited significant cellular adhesion and excellent biocompatibility in the *in vitro* studies.

The most effective approach for producing this composite has yet to be ascertained, including the parameters for a particular procedure or the fabrication techniques for producing appropriate structures. Only a few articles establish the optimal concentration of BT to be used in the composite. Each approach specifies a distinct quantity of ceramic material that differs from the other method. The investigation of the degradability of BT-PCL has not been explored yet. The existing methodologies, which include the utilisation of BT-PCL composites, typically require careful adjustment to optimise the desired structure for a particular application. There is a need for comprehensive investigations regarding the utilisation of this composite in the *in vivo* investigations. Additionally, further research is warranted to examine the impact of this composite on bacterial organisms. Furthermore, it is imperative to explore the mechanical characteristics of the composite, evaluate its potential as a material for dental implants, assess its viability as a coating material and investigate the influence of BT and PCL concentrations on the compound's adhesion to the implant.

## **Conclusion**

The PCL, BT and their associated composites exhibit excellent activity against bacteria with minimum cytotoxicity effect. PCL-BT composites combine good mechanical, piezoelectric and biological properties to accelerate the osseointegration and the overall healing process. PCL and BT show promising properties for biomedical applications, but further investigation is needed in the future.

## **Acknowledgements**

The authors would like to thank Baghdad University ([www.uobaghdad.edu.iq](http://www.uobaghdad.edu.iq)) and Mustansiriyah University ([www.uomustansiriyah.edu.iq](http://www.uomustansiriyah.edu.iq)) Baghdad- Iraq, for their support in the present work.



## Declaration of conflicting interests

The author(s) declared no potential conflicts of interest with respect to the research, authorship, and/or publication of this article.

## Funding

The author(s) received no financial support for the research, authorship, and/or publication of this article.

## ORCID iD

Sabreen Waleed Ibrahim  <https://orcid.org/0000-0002-8061-7662>

## References

1. Haberstroh K, Ritter K, Kuschnierz J, et al. Bone repair by cell-seeded 3D-bioplotting composite scaffolds made of collagen treated tricalciumphosphate or tricalciumphosphate-chitosan-collagen hydrogel or PLGA in ovine critical-sized calvarial defects. *J Biomed Mater Res Part B Appl Biomater* 2010; 93: 520–530.
2. Gómez-Lizárraga KK, Flores-Morales C, Del Prado-Audelo ML, et al. Polycaprolactone-and polycaprolactone/ceramic-based 3D-bioplotting porous scaffolds for bone regeneration: a comparative study. *Mater Sci Eng C* 2017; 79: 326–335.
3. Ghorbani FM, Kaffashi B, Shokrollahi P, et al. Effect of hydroxyapatite nanoparticles on morphology, rheology and thermal behavior of poly (caprolactone)/chitosan blends. *Mater Sci Eng C* 2016; 59: 980–989.
4. Mohammed AA and Hamad TI. Assessment of coating zirconium implant material with nanoparticles of faujasite. *J Baghdad Coll Dent* 2021; 33: 25–30.
5. Jani GH and Fatalla AA. Surface characterization of PEKK modified by strontium–hydroxyapatite coating as implant material via the magnetron sputtering deposition technique. *J Baghdad Coll Dent* 2022; 34: 25–36.
6. Mohammed DH and Jassim RK. Optimizing the surface properties of zirconium implants with germanium coating. *J Biomimetics, Biomater Biomed Eng* 2023; 59: 91–105.
7. Makhlof ASH and Abu-Thabit NY. *Advances in smart coatings and thin films for future Industrial and Biomedical Engineering Applications*. Elsevier, 2019. ISBN: 9780128118931.
8. Hivechi A, Bahrami SH, Siegel RA, et al. Cellulose nanocrystal effect on crystallization kinetics and biological properties of electrospun polycaprolactone. *Mater Sci Eng C* 2021; 121: 111855.
9. Salernitano E and Migliaresi C. Composite materials for biomedical applications: a review. *J Appl Biomater Biomech* 2003; 1: 3–18.
10. Juliadmi D, Tjong DH and Manjas M. The effect of sintering temperature on bilayers hydroxyapatite coating of Titanium (ti-6Al-4V) ELI by electrophoretic deposition for improving osseointegration. In: *IOP conference series: Materials science and engineering*. Indonesia: IOP Publishing, 2019, pp.12005.
11. Kim H-W, Lee E-J, Kim H-E, et al. Effect of fluoridation of hydroxyapatite in hydroxyapatite-polycaprolactone composites on osteoblast activity. *Biomaterials* 2005; 26: 4395–4404.
12. Kliem S, Kreutzbruck M and Bonten C. Review on the biological degradation of polymers in various environments. *Materials (Basel)* 2020; 13: 4586.

13. Dziadek M, Stodolak-Zych E and Cholewa-Kowalska K. Biodegradable ceramic-polymer composites for biomedical applications: a review. *Mater Sci Eng C* 2017; 71: 1175–1191.
14. Mohamed RM and Yusoh K. A review on the recent research of polycaprolactone (PCL). *Adv Mater Res* 2016; 1134: 249–255.
15. Nair LS and Laurencin CT. Biodegradable polymers as biomaterials. *Prog Polym Sci* 2007; 32: 762–798.
16. Van der Schueren L, De Schoenmaker B, Kalaoglu ÖI, et al. An alternative solvent system for the steady state electrospinning of polycaprolactone. *Eur Polym J* 2011; 47: 1256–1263.
17. Dwivedi R, Kumar S, Pandey R, et al. Polycaprolactone as biomaterial for bone scaffolds: review of literature. *J Oral Biol Craniofac Res* 2020; 10: 381–388.
18. He Y, Wildman RD, Tuck CJ, et al. An investigation of the behavior of solvent based polycaprolactone ink for material jetting. *Sci Rep* 2016; 6: 20852.
19. Zhang S, Campagne C and Salaün F. Influence of solvent selection in the electrospinning process of polycaprolactone. *Appl Sci* 2019; 9: 402.
20. Manivasagam G, Reddy A, Sen D, et al. Dentistry: Restorative and regenerative approaches. 2019.
21. Cipitria A, Skelton A, Dargaville TR, et al. Design, fabrication and characterization of PCL electrospun scaffolds—a review. *J Mater Chem* 2011; 21: 9419–9453.
22. Rocha J, Araújo JC, Figueiro R, et al. Wetspun polymeric fibrous systems as potential scaffolds for tendon and ligament repair, healing and regeneration. *Pharmaceutics* 2022; 14: 2526.
23. Dias JR, Sousa A, Augusto A, et al. Electrospun polycaprolactone (PCL) degradation: an in vitro and in vivo study. *Polymers (Basel)* 2022; 14: 3397.
24. Lam CXF, Huttmacher DW, Schantz J, et al. Evaluation of polycaprolactone scaffold degradation for 6 months in vitro and in vivo. *J Biomed Mater Res A*. 2009; 90: 906–919.
25. Shoja M, Shameli K, Ahmad MB, et al. Preparation, characterization and antibacterial properties of polycaprolactone/ZnO microcomposites. *Dig J Nanomater Biostructures* 2015; 10: 169–178.
26. Wang H, Synatschke CV, Raup A, et al. Oligomeric dual functional antibacterial polycaprolactone. *Polym Chem* 2014; 5: 2453–2460.
27. Yang Y, Zheng K, Liang R, et al. Cu-releasing bioactive glass/polycaprolactone coating on Mg with antibacterial and anticorrosive properties for bone tissue engineering. *Biomed Mater* 2017; 13: 15001.
28. Hajduga MB, Bobinski R, Dutka M, et al. The influence of graphene content on the antibacterial properties of polycaprolactone. *Int J Mol Sci* 2022; 23: 10899.
29. Augustine R, Malik HN, Singhal DK, et al. Electrospun polycaprolactone/ZnO nanocomposite membranes as biomaterials with antibacterial and cell adhesion properties. *J Polym Res* 2014; 21: 1–17.
30. Chen C-H, Chen S-H, Shalumon KT, et al. Dual functional core–sheath electrospun hyaluronic acid/polycaprolactone nanofibrous membranes embedded with silver nanoparticles for prevention of peritendinous adhesion. *Acta Biomater* 2015; 26: 225–235.
31. Gao Y, Hassanbhai AM, Lim J, et al. Fabrication of a silver octahedral nanoparticle-containing polycaprolactone nanocomposite for antibacterial bone scaffolds. *RSC Adv* 2017; 7: 10051–6.
32. Zeng A, Wang Y, Li D, et al. Preparation and antibacterial properties of polycaprolactone/quaternized chitosan blends. *Chinese J Chem Eng* 2021; 32: 462–471.
33. Balcucho J, Narváez DM and Castro-Mayorga JL. Antimicrobial and biocompatible polycaprolactone and copper oxide nanoparticle wound dressings against methicillin-resistant *Staphylococcus aureus*. *Nanomaterials* 2020; 10: 1692.

34. Lin W-C, Yao C, Huang T-Y, et al. Long-term in vitro degradation behavior and biocompatibility of polycaprolactone/cobalt-substituted hydroxyapatite composite for bone tissue engineering. *Dent Mater* 2019; 35: 751–762.
35. Martínez-Abad A, Sánchez G, Fuster V, et al. Antibacterial performance of solvent cast polycaprolactone (PCL) films containing essential oils. *Food Control* 2013; 34: 214–220.
36. Jang CH, Cho YB, Jang YS, et al. Antibacterial effect of electrospun polycaprolactone/polyethylene oxide/vancomycin nanofiber mat for prevention of periprosthetic infection and biofilm formation. *Int J Pediatr Otorhinolaryngol* 2015; 79: 1299–1305.
37. Hassan MI and Sultana N. Characterization, drug loading and antibacterial activity of nano-hydroxyapatite/polycaprolactone (nHA/PCL) electrospun membrane. *3 Biotech* 2017; 7: 249.
38. Radisavljevic A, Stojanovic DB, Perisic S, et al. Cefazolin-loaded polycaprolactone fibers produced via different electrospinning methods: characterization, drug release and antibacterial effect. *Eur J Pharm Sci* 2018; 124: 26–36.
39. Lim MM and Sultana N. In vitro cytotoxicity and antibacterial activity of silver-coated electrospun polycaprolactone/gelatin nanofibrous scaffolds. *3 Biotech* 2016; 6: 1–10.
40. Prado-Prone G, Silva-Bermudez P, Almaguer-Flores A, et al. Enhanced antibacterial nanocomposite mats by coaxial electrospinning of polycaprolactone fibers loaded with zn-based nanoparticles. *Nanomedicine* 2018; 14: 1695–1706.
41. Tursucular OF, Çerkez İ, Orhan M, et al. Preparation and antibacterial investigation of polycaprolactone/chitosan nano/micro fibers by using different solvent systems. *Text Appar* 2018; 28: 221–228.
42. Unalan I, Slavik B, Buettner A, et al. Physical and antibacterial properties of peppermint essential oil loaded poly ( $\epsilon$ -caprolactone)(PCL) electrospun fiber mats for wound healing. *Front Bioeng Biotechnol* 2019; 7: 346.
43. Ahmed J, Gultekinoglu M, Bayram C, et al. Alleviating the toxicity concerns of antibacterial cinnamon-polycaprolactone biomaterials for healthcare-related biomedical applications. *MedComm (2020)* 2021; 2: 236–246.
44. Cai Y, Guan J, Wang W, et al. Ph and light-responsive polycaprolactone/curcumin@ zif-8 composite films with enhanced antibacterial activity. *J Food Sci* 2021; 86: 3550–3562.
45. Alipour M, Pouya B, Aghazadeh Z, et al. The antimicrobial, antioxidative, and anti-inflammatory effects of polycaprolactone/gelatin scaffolds containing chrysin for regenerative endodontic purposes. *Stem Cells Int* 2021; 2021: 1–11.
46. Felgueiras HP, Homem NC, Teixeira MA, et al. Physical, thermal, and antibacterial effects of active essential oils with potential for biomedical applications loaded onto cellulose acetate/polycaprolactone wet-spun microfibers. *Biomolecules* 2020; 10: 1129.
47. Gámez E, Elizondo-Castillo H, Tascon J, et al. Antibacterial effect of thymol loaded SBA-15 nanorods incorporated in PCL electrospun fibers. *Nanomaterials* 2020; 10: 616.
48. Zhang Y, Chang M, Bao F, et al. Multifunctional Zn doped hollow mesoporous silica/polycaprolactone electrospun membranes with enhanced hair follicle regeneration and antibacterial activity for wound healing. *Nanoscale* 2019; 11: 6315–6333.
49. Angulo-Pineda C, Srirussamee K, Palma P, et al. Electroactive 3D printed scaffolds based on percolated composites of polycaprolactone with thermally reduced graphene oxide for antibacterial and tissue engineering applications. *Nanomaterials* 2020; 10: 428.
50. Ghosal K, Kováčová M, Humpolíček P, et al. Antibacterial photodynamic activity of hydrophobic carbon quantum dots and polycaprolactone based nanocomposite processed via both electrospinning and solvent casting method. *Photodiagnosis Photodyn Ther* 2021; 35: 102455.
51. Khunová V, Kováčová M, Olejníková P, et al. Antibacterial electrospun polycaprolactone nanofibers reinforced by halloysite nanotubes for tissue engineering. *Polymers (Basel)* 2022; 14: 746.

52. Musciacchio L, Mardirossian M, Guagnini B, et al. Rifampicin-loaded electrospun polycaprolactone membranes: characterization of stability, antibacterial effects and urotheliocytes proliferation. *Mater Des* 2022; 224: 111286.
53. Li T-T, Sun L, Zhong Y, et al. Silk fibroin/polycaprolactone-polyvinyl alcohol directional moisture transport composite film loaded with antibacterial drug-loading microspheres for wound dressing materials. *Int J Biol Macromol* 2022; 207: 580–591.
54. Soenen SJ, Manshian B, Montenegro JM, et al. Cytotoxic effects of gold nanoparticles: a multiparametric study. *ACS Nano* 2012; 6: 5767–5783.
55. De Melo WM, Maximiano WMA, Antunes AA, et al. Cytotoxicity testing of methyl and ethyl 2-cyanoacrylate using direct contact assay on osteoblast cell cultures. *J Oral Maxillofac Surg* 2013; 71: 35–41.
56. Li W, Zhou J and Xu Y. Study of the in vitro cytotoxicity testing of medical devices. *Biomed Reports* 2015; 3: 617–620.
57. Malikhhammadov E, Tanir TE, Kiziltay A, et al. PCL and PCL-based materials in biomedical applications. *J Biomater Sci Polym Ed* 2018; 29: 863–893.
58. Zander NE, Orlicki JA, Rawlett AM, et al. Quantification of protein incorporated into electrospun polycaprolactone tissue engineering scaffolds. *ACS Appl Mater Interfaces* 2012; 4: 2074–2081.
59. Lee SJ, Won J-E, Han C, et al. Development of a three-dimensionally printed scaffold grafted with bone forming peptide-1 for enhanced bone regeneration with in vitro and in vivo evaluations. *J Colloid Interface Sci* 2019; 539: 468–480.
60. Ho C, Fang H, Wang B, et al. The effects of Biodentine/polycaprolactone three-dimensional-scaffold with odontogenesis properties on human dental pulp cells. *Int Endod J* 2018; 51: e291–e300.
61. Fedore CW, Tse LYL, Nam HK, et al. Analysis of polycaprolactone scaffolds fabricated via precision extrusion deposition for control of craniofacial tissue mineralization. *Orthod Craniofac Res* 2017; 20: 12–17.
62. Cunha Dd, Inforçatti Neto P, Micocci KC, et al. Fabrication and characterization of scaffolds of poly ( $\epsilon$ -caprolactone)/Biosilicate® biocomposites prepared by generative manufacturing process. *Int J Biomater* 2019; 2019: 1–11.
63. Wei L-G, Chang H-I, Wang Y, et al. A gelatin/collagen/polycaprolactone scaffold for skin regeneration. *PeerJ* 2019; 7: e6358.
64. Safi IN, Al-Shammari AM, Ul-Jabbar MA, et al. Preparing polycaprolactone scaffolds using electrospinning technique for construction of artificial periodontal ligament tissue. *J Taibah Univ Med Sci* 2020; 15: 363–373.
65. Son S-R, Linh N-TB, Yang H-M, et al. In vitro and in vivo evaluation of electrospun PCL/PMMA fibrous scaffolds for bone regeneration. *Sci Technol Adv Mater* 2013; 14: 1–10.
66. Teo EY, Ong S-Y, Chong MSK, et al. Polycaprolactone-based fused deposition modeled mesh for delivery of antibacterial agents to infected wounds. *Biomaterials* 2011; 32: 279–287.
67. Swami V, Vijayaraghavan V and Swami V. Current trends to measure implant stability. *J Indian Prosthodont Soc* 2016; 16: 124.
68. Fu X, Sammons RL, Bertóti I, et al. Atomic layer deposition plasma surface modification of polycaprolactone to improve cell attachment. *J Biomed Mater Res B Appl Biomater* 2012; 100: 314–320.
69. Jiang J, Xie J, Ma B, et al. Mussel-inspired protein-mediated surface functionalization of electrospun nanofibers for pH-responsive drug delivery. *Acta Biomater* 2014; 10: 1324–1332.
70. Lino AB, McCarthy AD and Fernández JM. Evaluation of strontium-containing PCL-PDIPF scaffolds for bone tissue engineering: in vitro and in vivo studies. *Ann Biomed Eng* 2019; 47: 902–912.

71. Hwang TI, Kim JI, Joshi MK, et al. Simultaneous regeneration of calcium lactate and cellulose into PCL nanofiber for biomedical application. *Carbohydr Polym* 2019; 212: 21–29.
72. Lee SJ, Lee D, Yoon TR, et al. Surface modification of 3D-printed porous scaffolds via mussel-inspired polydopamine and effective immobilization of rhBMP-2 to promote osteogenic differentiation for bone tissue engineering. *Acta Biomater* 2016; 40: 182–191.
73. Seyednejad H, Gawlitta D, Dhert WJA, et al. Preparation and characterization of a three-dimensional printed scaffold based on a functionalized polyester for bone tissue engineering applications. *Acta Biomater* 2011; 7: 1999–2006.
74. Spalthoff S, Zimmerer R, Dittmann J, et al. Scapula pre-augmentation in sheep with polycaprolactone tricalcium phosphate scaffolds. *J Stomatol Oral Maxillofac Surg* 2019; 120: 116–121.
75. Xiang P, Li M, Zhang C, et al. Cytocompatibility of electrospun nanofiber tubular scaffolds for small diameter tissue engineering blood vessels. *Int J Biol Macromol* 2011; 49: 281–288.
76. Chen G, Zhou P, Mei N, et al. Silk fibroin modified porous poly ( $\epsilon$ -caprolactone) scaffold for human fibroblast culture in vitro. *J Mater Sci Mater Med* 2004; 15: 671–677.
77. Bao T-Q, Franco RA and Lee B-T. Preparation and characterization of a novel 3D scaffold from poly ( $\epsilon$ -caprolactone)/biphasic calcium phosphate hybrid composite microspheres adhesion. *Biochem Eng J* 2012; 64: 76–83.
78. Li L, Qian Y, Jiang C, et al. The use of hyaluronan to regulate protein adsorption and cell infiltration in nanofibrous scaffolds. *Biomaterials* 2012; 33: 3428–3445.
79. Savarino L, Baldini N, Greco M, et al. Polycaprolactone (PCL) scaffolds in tissue engineering research. *Bone* 2008; 4: 381–388.
80. Chuenjitkuntaworn B, Inrung W, Damrongsri D, et al. Polycaprolactone/hydroxyapatite composite scaffolds: preparation, characterization, and in vitro and in vivo biological responses of human primary bone cells. *J Biomed Mater Res A* 2010; 94: 241–251.
81. Pilipchuk SP, Monje A, Jiao Y, et al. Integration of 3D printed and micropatterned polycaprolactone scaffolds for guidance of oriented collagenous tissue formation in vivo. *Adv Healthc Mater* 2016; 5: 676–687.
82. Eftekhari H, Jahandideh A, Asghari A, et al. Histopathological evaluation of polycaprolactone nanocomposite compared with tricalcium phosphate in bone healing. *J Vet Res* 2018; 62: 385.
83. Rashid M, Dudhia J, Dakin SG, et al. Histopathological and immunohistochemical evaluation of cellular response to a woven and electrospun polydioxanone (PDO) and polycaprolactone (PCL) patch for tendon repair. *Sci Rep* 2020; 10: 4754.
84. Dębski T, Wysocki J, Siennicka K, et al. Modified histopathological protocol for poly- $\epsilon$ -caprolactone scaffolds preserving their trabecular, honeycomb-like structure. *Materials (Basel)* 2022; 15: 1732.
85. Shahrezaee M, Salehi M, Keshtkari S, et al. In vitro and in vivo investigation of PLA/PCL scaffold coated with metformin-loaded gelatin nanocarriers in regeneration of critical-sized bone defects. *Nanomedicine* 2018; 14: 2061–2073.
86. Samadian H, Ehterami A, Sarrafzadeh A, et al. Sophisticated polycaprolactone/gelatin nanofibrous nerve guided conduit containing platelet-rich plasma and citicoline for peripheral nerve regeneration: in vitro and in vivo study. *Int J Biol Macromol* 2020; 150: 380–388.
87. Acosta M, Novak N, Rojas V, et al. BaTiO<sub>3</sub>-based piezoelectrics: fundamentals, current status, and perspectives. *Appl Phys Rev* 2017; 4: 41305.
88. Gao T, Liao J, Wang J, et al. Highly oriented BaTiO<sub>3</sub> film self-assembled using an interfacial strategy and its application as a flexible piezoelectric generator for wind energy harvesting. *J Mater Chem B* 2015; 3: 9965–9971.
89. Jiang B, Iocozzia J, Zhao L, et al. Barium titanate at the nanoscale: controlled synthesis and dielectric and ferroelectric properties. *Chem Soc Rev* 2019; 48: 1194–1228.

90. Scott JF. Dimensional effects on ferroelectrics: ultra-thin single crystals, nanotubes, nano-rods, and nano-ribbons. *Ferroelectrics* 2005; 316: 13–21.
91. Buscaglia V and Randall CA. Size and scaling effects in barium titanate. An overview. *J Eur Ceram Soc* 2020; 40: 3744–3758.
92. Fan B, Guo Z, Li X, et al. Electroactive barium titanate coated titanium scaffold improves osteogenesis and osseointegration with low-intensity pulsed ultrasound for large segmental bone defects. *Bioact Mater* 2020; 5: 1087–1101.
93. Liu B, Chen L, Shao C, et al. Improved osteoblasts growth on osteomimetic hydroxyapatite/BaTiO<sub>3</sub> composites with aligned lamellar porous structure. *Mater Sci Eng C* 2016; 61: 8–14.
94. Radzi MHM and Leong KS. Investigation of the piezoelectric charge coefficient d<sub>33</sub> of thick-film piezoelectric ceramics by varying poling and repoling conditions. In: *AIP Conference proceedings*. Malaysia: AIP Publishing LLC, 2015, pp.70083.
95. Nuraje N and Su K. Perovskite ferroelectric nanomaterials. *Nanoscale* 2013; 5: 8752–8780.
96. Lin C-M and Yen SK. Biocompatibility and corrosion behavior of BaTiO<sub>3</sub>/TiO<sub>2</sub> double layers by electrochemical synthesis. *Key Eng Mater.* 2006; 309–311: 371–374.
97. Sinaei M, Heidari F and Hayati R. Investigation of corrosion properties of nanocomposite coatings of hydroxyapatite/barium titanate/chitosan produced by electrophoretic deposition on 316L stainless steel. *Surf Eng Appl Electrochem* 2020; 56: 272–281.
98. Ciobanu CS, Iconaru SL, Le Coustumer P, et al. Antibacterial activity of silver-doped hydroxyapatite nanoparticles against gram-positive and gram-negative bacteria. *Nanoscale Res Lett* 2012; 7: 1–9.
99. Singh A and Dubey AK. Various biomaterials and techniques for improving antibacterial response. *ACS Appl Bio Mater* 2018; 1: 3–20.
100. Swain S and Rautray TR. Silver doped hydroxyapatite coatings by sacrificial anode deposition under magnetic field. *J Mater Sci Mater Med* 2017; 28: 1–5.
101. Munisparan T, Yang ECY, Paramasivam R, et al. Optimisation of preparation conditions for ti nanowires and suitability as an antibacterial material. *IET Nanobiotechnol* 2018; 12: 429–435.
102. Yao T, Chen J, Wang Z, et al. The antibacterial effect of potassium-sodium niobate ceramics based on controlling piezoelectric properties. *Colloids Surf B Biointerfaces* 2019; 175: 463–468.
103. Swain S, Padhy RN and Rautray TR. Polarized piezoelectric bioceramic composites exhibit antibacterial activity. *Mater Chem Phys* 2020; 239: 122002.
104. Sabourian P, Yazdani G, Ashraf SS, et al. Effect of physico-chemical properties of nanoparticles on their intracellular uptake. *Int J Mol Sci* 2020; 21: 8019.
105. Singh N, Marets C, Boudon J, et al. In vivo protein corona on nanoparticles: does the control of all material parameters orient the biological behavior? *Nanoscale Adv* 2021; 3: 1209–1229.
106. Shah AA, Khan A, Dwivedi S, et al. Antibacterial and antibiofilm activity of barium titanate nanoparticles. *Mater Lett* 2018; 229: 130–133.
107. Sasikumar M, Ganeshkumar A, Chandraprabha MN, et al. Investigation of antimicrobial activity of CTAB assisted hydrothermally derived Nano BaTiO<sub>3</sub>. *Mater Res Express* 2018; 6: 25408.
108. Boschetto F, Doan HN, Phong Vo P, et al. Bacteriostatic behavior of PLA-BaTiO<sub>3</sub> composite fibers synthesized by centrifugal spinning and subjected to aging test. *Molecules* 2021; 26: 2918.
109. Shuai C, Liu G, Yang Y, et al. A strawberry-like Ag-decorated barium titanate enhances piezoelectric and antibacterial activities of polymer scaffold. *Nano Energy* 2020; 74: 104825.
110. Marin E, Mukai M, Boschetto F, et al. Antibacterial 3D-printed PMMA/ceramic composites. *bioRxiv* 2021; 10: 2010–2021.

111. Marin E, Boschetto F, Sunthar TPM, et al. Antibacterial effects of barium titanate reinforced polyvinyl-siloxane scaffolds. *Int J Polym Mater Polym Biomater* 2021; 70: 425–436.
112. Zaichick V, Zaichick S, Karandashev V, et al. The effect of age and gender on Al, B, Ba, Ca, Cu, Fe, K, Li, Mg, Mn, Na, P, S, Sr, V, and Zn contents in rib bone of healthy humans. *Biol Trace Elem Res* 2009; 129: 107–115.
113. Zheng T, Zhao H, Huang Y, et al. Piezoelectric calcium/manganese-doped barium titanate nanofibers with improved osteogenic activity. *Ceram Int* 2021; 47: 28778–28789.
114. Ahamed M, Akhtar MJ, Khan MAM, et al. Barium titanate (BaTiO<sub>3</sub>) nanoparticles exert cytotoxicity through oxidative stress in human lung carcinoma (A549) cells. *Nanomaterials* 2020; 10: 2309.
115. Zhu P, Chen Y and Shi J. Piezocatalytic tumor therapy by ultrasound-triggered and BaTiO<sub>3</sub>-mediated piezoelectricity. *Adv Mater* 2020; 32: 2001976.
116. Staedler D, Magouroux T, Hadji R, et al. Harmonic nanocrystals for biolabeling: a survey of optical properties and biocompatibility. *ACS Nano* 2012; 6: 2542–2549.
117. Sood A, Desseigne M, Dev A, et al. A comprehensive review on barium titanate nanoparticles as a persuasive piezoelectric material for biomedical applications: prospects and challenges. *Small* 2023; 19: 2206401.
118. Bonacina L. Nonlinear nanomedicine: harmonic nanoparticles toward targeted diagnosis and therapy. *Mol Pharm* 2013; 10: 783–792.
119. Marino A, Genchi GG, Sinibaldi E, et al. Piezoelectric effects of materials on bio-interfaces. *ACS Appl Mater Interfaces* 2017; 9: 17663–17680.
120. Cafarelli A, Marino A, Vannozzi L, et al. Piezoelectric nanomaterials activated by ultrasound: the pathway from discovery to future clinical adoption. *ACS Nano* 2021; 15: 11066–11086.
121. Ciofani G, Danti S, D'Alessandro D, et al. Barium titanate nanoparticles: highly cytocompatible dispersions in glycol-chitosan and doxorubicin complexes for cancer therapy. *Nanoscale Res Lett* 2010; 5: 1093–1101.
122. Zhang Y, Chen L, Zeng J, et al. Aligned porous barium titanate/hydroxyapatite composites with high piezoelectric coefficients for bone tissue engineering. *Mater Sci Eng C* 2014; 39: 143–149.
123. Shokrollahi H, Salimi F and Doostmohammadi A. The fabrication and characterization of barium titanate/akermanite nano-bio-ceramic with a suitable piezoelectric coefficient for bone defect recovery. *J Mech Behav Biomed Mater* 2017; 74: 365–370.
124. Busuioc C, Voicu G, Jinga S-I, et al. The influence of barium titanate on the biological properties of collagen-hydroxyapatite composite scaffolds. *Mater Lett* 2019; 253: 317–322.
125. Rahmati S, Basiriani MB, Rafienia M, et al. Synthesis and in vitro evaluation of electrodeposited Barium titanate coating on Ti6Al4 V. *J Med Signals Sens* 2016; 6: 106.
126. Tang Y, Wu C, Zhang P, et al. Degradation behaviour of non-sintered graphene/barium titanate/magnesium phosphate cement bio-piezoelectric composites. *Ceram Int* 2020; 46: 12626–12636.
127. Vandrovцова M, Tolde Z, Vanek P, et al. Beta-Titanium alloy covered by ferroelectric coating—physicochemical properties and human osteoblast-like cell response. *Coatings* 2021; 11: 210.
128. Lopes HB, Santos TdS, de Oliveira FS, et al. Poly (vinylidene-trifluoroethylene)/barium titanate composite for in vivo support of bone formation. *J Biomater Appl* 2014; 29: 104–112.
129. Dai X, Yao X, Zhang W, et al. The osteogenic role of barium titanate/poly(lactic acid) piezoelectric composite membranes as guiding membranes for bone tissue regeneration. *Int J Nanomedicine* 2022; 17: 4339–4353.
130. Sikder P, Nagaraju P and Naganaboyina HPS. 3D-printed piezoelectric porous bioactive scaffolds and clinical ultrasonic stimulation can help in enhanced bone regeneration. *Bioengineering* 2022; 9: 679.

131. Liu J, Gu H, Liu Q, et al. An intelligent material for tissue reconstruction: the piezoelectric property of polycaprolactone/barium titanate composites. *Mater Lett* 2019; 236: 686–689.
132. Tang Y, Wu C, Wu Z, et al. Fabrication and in vitro biological properties of piezoelectric bioceramics for bone regeneration. *Sci Rep* 2017; 7: 43360.
133. Tavangar M, Heidari F, Hayati R, et al. Manufacturing and characterization of mechanical, biological and dielectric properties of hydroxyapatite-barium titanate nanocomposite scaffolds. *Ceram Int* 2020; 46: 9086–9095.
134. Baxter FR, Turner IG, Bowen CR, et al. An in vitro study of electrically active hydroxyapatite-barium titanate ceramics using Saos-2 cells. *J Mater Sci Mater Med* 2009; 20: 1697–1708.
135. Rezaie HR, Rizi HB, Khamseh MMR, et al. *Iran. A review on dental materials*. Springer, 2020.
136. Sgarminato V. Composite scaffolds with porosity over multiple length scales for skin regeneration, thesis. *Politecnico di Torino* 2018.
137. Ibrahim SW and Hamad TI. Electrospun nano-barium titanate/polycaprolactone composite coatings on titanium and Ti13Nb13Zr alloy. *Compos Adv Mater* 2023: 32.

### Author biographies

Sabreen Waleed Ibrahim is Lecturer in Prosthodontic, her area of research in advanced and composite materials, coatings deposition and characterization, implants surface treatment and esthetics.

Thekra Ismael Hamad is Prof in Prosthodontic, her area of research in materials and implants.

Julfikar Haider is Senior Lecturer in Engineering, his area of research in composite materials, surface engineering, Tribology, metal casting, metal cutting machining, advanced welding, manufacturing systems, artificial intelligence, and finite element modelling.